

Lower Leg Joint Strategies in the Outside Pass in Soccer

Yudai Yamamoto¹^a, Viktor Kozák²^b and Ikuo Mizuuchi³^c

¹Department of Food and Energy Systems Science, Tokyo University of Agriculture and Technology, Naka-cho 2-24-16, Koganei-shi 184-0012, Tokyo-to, Japan

²Czech Institute of Informatics, Robotics, and Cybernetics, Czech Technical University in Prague, Jugoslávských Partyzánů 1580/3, 160 00 Praha 6, Czech Republic

³Department of Mechanical Systems Engineering, Tokyo University of Agriculture and Technology, Naka-cho 2-24-16, Koganei-shi 184-0012, Tokyo-to, Japan

Keywords: Medial Collateral Ligament, Lateral Collateral Ligament, Outside Pass, Strategies, Reinforcement Learning.

Abstract: We study the leg motion for an outside pass in soccer, observing four different movement strategies. The aim of this research is to validate the presence of these four strategies by training an agent with a higher reward for kicking a faster ball. Additionally, we aim to explore the role of the collateral ligaments' stiffness in the outside pass. We built two leg models: (a) a two-degree-of-freedom leg model that applies torque around the hip joint, and (b) a three-degree-freedom leg model that applies pitch-roll-yaw torque around the hip joint and pitch torque around the knee joint. We trained a Deep Deterministic Policy Gradient (DDPG) agent using these models and analyzed the torques around the hip and knee joints, as well as the ball velocity after the leg loses contact with the ball. We observed three strategies similar to human behavior throughout agent learning.

1 INTRODUCTION


There are various types of passes in soccer, and each pass is determined based on strategies. When focusing on an outside pass without curve – where the ball is kicked with the outside of the foot – we observe four strategies: pulling the thigh backward diagonally, bending the knee, stopping the thigh's acceleration, and stretching the knee suddenly. (Fig. 1). The body motion can be studied using a mechanism embedded in the human body called kinetic chain. The transmission of the accumulated energy through kinetic links and radiated energy at the time of ball throw is demonstrated in (Senoo et al., 2008). The human body has ability to store potential energy using its elasticity (Chiras, 2018)(Ker et al., 1987)(Woo et al., 1993)(Levin et al., 1927). We hypothesize that ligament elasticity plays a role in energy accumulation during the backward swing of the leg. For swing motion, using a robot by stopping the base link and accelerating the end link is realized (Xu et al., 2007).


Furthermore, the use of elastic joint oscillation to throw a faster ball by increasing the mechanical en-




Figure 1: Four strategies of an outside pass in soccer are as follows:(1-1) Pulling the thigh backward diagonally rotating the hip joint around the roll-pitch-yaw axes and the knee joint around the roll-pitch axes, (1-2) Bending the knee rotating knee joint around the pitch axis, (2-1) Stopping the thigh's acceleration rotating the hip joint around the roll axis , and (2-2) Stretching the knee suddenly rotating the knee joint around the pitch axis.

ergy has been demonstrated (Hondo and Mizuuchi, 2012). We assume that ligaments facilitate the exchange of kinetic and potential energy between the thigh and shin, enabling the leg movement to efficiently convert into the shin's kinetic energy. Studies on muscle tendon utilization during kicking (Cerrah et al., 2011) , jumping (Fukasawa, 2000), and step-

^a <https://orcid.org/0009-0004-1961-1992>

^b <https://orcid.org/0000-0001-8405-269X>

^c <https://orcid.org/0000-0003-4657-2613>

ping (Wiesinger et al., 2017)(Aeles and Vanwanseele, 2019) highlight the role of elastic elements. However, research specifically focusing on ligament in sports activities remains limited. In the case of an outside pass, kicking the ball with the outside of the foot may cause knee oscillation around the roll axis. The goal of our research is to validate the presence of four strategies in reinforcement learning agent with kicking faster ball higher reward. Furthermore, we aim to reveal the roles of collateral ligaments located on medial and lateral side of the knee in an outside pass in soccer.

2 THE STRATEGIES

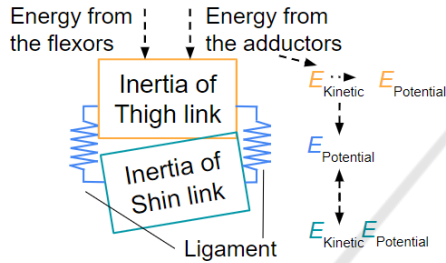


Figure 2: The four strategies collectively increase the kinetic energy of the shin, directing it towards the ball.

The rotational stiffness of the knee joint having two collateral ligaments is non-linear. However for the purpose of this research, the difference between non-linear and linear joint stiffness is negligible. We modeled the knee joint as two rigid links connected by a torsional linear spring. The system's equation of motion can be expressed as:

$$\mathbf{M}(\mathbf{q})\ddot{\mathbf{q}} + \mathbf{c}(\mathbf{q}, \dot{\mathbf{q}}) - \boldsymbol{\tau}_g(\mathbf{q}) = \boldsymbol{\tau}_p(\mathbf{q}, \dot{\mathbf{q}}) + \mathbf{u} \quad (1)$$

where $\mathbf{q} \in \mathbb{R}^3$ represents the generalized coordinates. $\mathbf{M}(\mathbf{q})$ is the 3×3 inertia matrix, and $\mathbf{c}(\mathbf{q}, \dot{\mathbf{q}}) \in \mathbb{R}^3$ is the Coriolis matrix. The terms $\boldsymbol{\tau}_g(\mathbf{q})$ and $\boldsymbol{\tau}_p(\mathbf{q}, \dot{\mathbf{q}})$ are 3-dimensional vectors representing external joint torques due to gravity, elasticity, and viscosity. Lastly, \mathbf{u} is the input torque vector. The total energy of translational and rotational kinetic energy $K(\mathbf{q}, \dot{\mathbf{q}})$, the gravitational potential energy of the thigh and shin $U_{Gravity}(\mathbf{q})$, and the ligament elastic potential energy $U_{Elastic}(\mathbf{q})$ are expressed as follows:

$$K(\mathbf{q}, \dot{\mathbf{q}}) = \frac{1}{2} \mathbf{v}_{COM}^T \mathbf{m} \mathbf{v}_{COM} + \frac{1}{2} \boldsymbol{\omega}^T \mathbf{I} \boldsymbol{\omega} \quad (2)$$

$$U_{Gravity}(\mathbf{q}) = -mgh \quad (3)$$

$$U_{Elastic}(\mathbf{q}) = \frac{1}{2} k \boldsymbol{\theta}^2 \quad (4)$$

where m is the mass, \mathbf{v}_{COM} is the center of mass (COM) velocity, $\boldsymbol{\omega}$ is the angular velocity, \mathbf{I} is the inertia tensor, h is the COM height, k is the knee stiffness around roll axis, and $\boldsymbol{\theta}$ is the knee roll angle. Fig. 2 illustrates the energy flow between the thigh and shin. Energy from the hip joint adductors and knee joint flexors is transferred into the kinetic and potential energy of the thigh, K_{Thigh} and U_{Thigh} (Pulling the thigh backward diagonally and bending the knee). This increases the kinetic energy and initiates the kinetic chain. At the same time the hip joint rotates around yaw axis to guide the kinetic energy toward the ball. Hip abduction and flexion are small, with most of the energy goes to thigh's kinetic energy, K_{Thigh} . This kinetic energy K_{Thigh} then converted into the potential energy of the ligaments and muscle-tendon complex. By suddenly stopping the motion of the hip joint along the roll, pitch, and yaw axes, the kinetic energy is transferred to the lower leg (Stopping the thigh's acceleration). Consequently, this action causes the knee joint to accelerate toward the ball (Stretching the knee suddenly). After striking the ball, the leg does not swing through, reducing the thigh's kinetic energy, K_{Thigh} , and increasing the shin's kinetic energy, K_{Shin} , and its potential energy due to gravity, U_{Shin} . These four strategies collectively work to increase the shin's kinetic energy, K_{Shin} , and resulting in a faster ball. Taking the derivative of the kinetic energy in Eq. (2) with respect to time t yields:

$$\dot{K} = \dot{\mathbf{v}}_{COM}^T \mathbf{m} \mathbf{v}_{COM} + \boldsymbol{\omega}^T \mathbf{I} \dot{\boldsymbol{\omega}} \quad (5)$$

The factors influencing the change in kinetic energy (K_{Shin}) during swing motion have been studied to explore methods for increasing the kinetic energy of the end link (Asaoka and Mizuuchi, 2017). Elements such as angular acceleration, angular velocity, and the moment arm affect the energy transfer rate within the leg. Studies on throwing (Tomohisa et al., 1997)(Kozo and Takeo, 2006) and kicking motions (Kozo et al., 2007) have examined the energy flow. Regardless of the scale of motion, even in outside pass, the acceleration and deceleration of the leg ensure that kinetic energy flows from the thigh to the shin.

3 METHODS

We determined the spring constant of the knee joint around the roll axis based on the human parameters (Table 1). Using reinforcement learning, we explicitly can decide a cost function for four strategies, such as kicking a faster ball quickly. The reward function

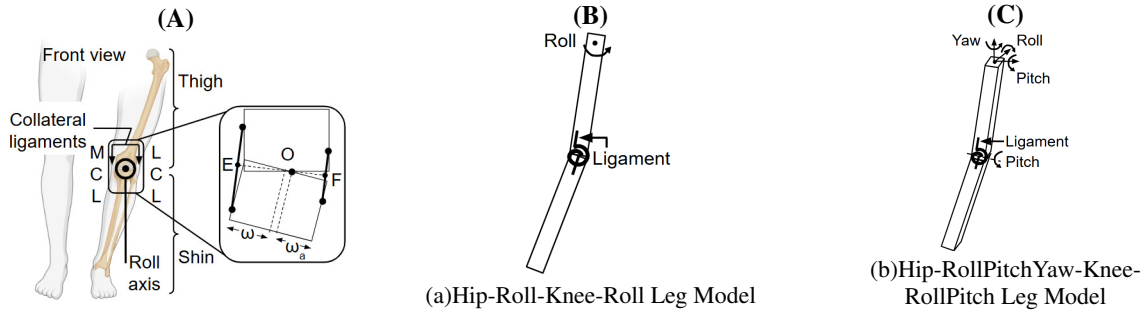


Figure 3: The medial collateral ligament (MCL) and lateral collateral ligament (LCL) are attached to the medial and lateral sides of the knee joint. The stiffness of these ligaments is approximated as linear torsional stiffness for knee's roll axis in both (a) and (b).

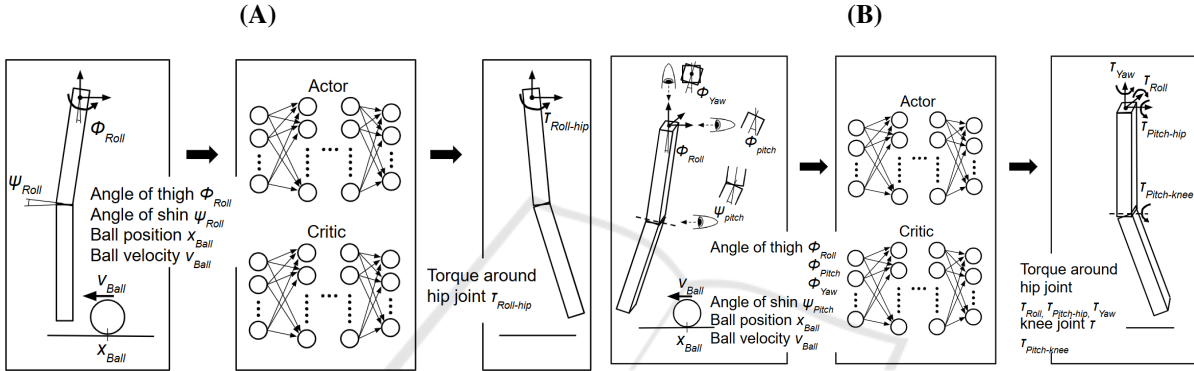


Figure 4: (A) The DDPG neural network model determines the torque input around the hip joint's roll axis in knee model (a), based on the angles of thigh and shin, the ball's position, and its velocity. (B) The DDPG neural network model determines the torque inputs around the hip and knee joints in knee model (b), based on the angles of the thigh and shin, the ball's position, and its velocity.

Table 1: Parameters of the leg and the ball (Ishii et al., 2009; Herman, 2009; Ho-Jung and Dai-Soon, 2020; Christenson and Casa, 2020; Nagurka et al., 2004).

Parameters	Values
m_{Thigh}	7 kg
m_{Shin}	3.26 kg
m_{Ball}	0.43 kg
h_{Thigh}	0.4214 m
h_{Shin}	0.4231 m
w	0.0225 m
w_a	0.0147 m
l_{MCL}	68.99×10^{-3} m
l_{LCL}	48.15×10^{-3} m
k_{MCL}	71.97×10^3 N/m
k_{LCL}	69.70×10^3 N/m
k_{Ball}	10.88×10^3 N/m

was designed to ensure that the ball's velocity after impact is faster and that the range of motion of the hip and knee joints remains within human limits (Table 2). Under these conditions, we evaluated whether the agent could gain a state-based action for the four strategies.

Table 2: Human joint angle and torque limits.

	Angle [deg]	Torque [N · m]
Hip Joint		
Flexion	132	105
Extension	15	158
Abduction	46	112
Adduction	23	76
Internal	38	84
External	46	67
Knee Joint		
Flexion	154	126
Extension	0	229

3.1 Knee Joint Stiffness of Abduction and Adduction

To simplify knee stiffness, we approximate the knee as having a torsion spring instead of modeling it with two ligaments. (Fig. 3(A)) Equating the potential energy of the ligaments to that of torsion spring gives us

$$\frac{1}{2}k\theta^2 = \frac{1}{2}k_{MCL}\Delta l_{MCL}^2 + \frac{1}{2}k_{LCL}\Delta l_{LCL}^2 \quad (6)$$

where k represents the torsion spring constant, and θ is the small flexion angle around the roll axis. k_{MCL} and k_{LCL} are the stiffness values of the two ligaments, while Δl_{MCL} and Δl_{LCL} represent the elongations from natural lengths. For small angles θ , $\Delta l_{MCL} \approx |OE|\theta$, $\Delta l_{LCL} \approx |OF|\theta$, where $|OE|$ and $|OF|$ are the moment arms illustrated in Fig. 3(A).

$$K = k_{MCL}|OE|^2 + k_{LCL}|OF|^2 \quad (7)$$

Assuming small values for θ , $|OE|$ and $|OF|$ can be considered constant: $|OE|^2 = 2w^2(1 - w_a)^2 + (l_{MCL}^2/2)$ and $|OF|^2 = 2w^2w_a^2 + (l_{LCL}^2/2)$, where l_{MCL} and l_{LCL} are the natural lengths of each ligament. Using this approximation, the knee joint stiffness is about 137 Nm/rad.

3.2 Leg and Leg-Ball Contact Model

We used two types of leg models: (a) Hip-Roll-Knee-Roll Leg Model (Fig. 3(B)) and (b) Hip-PitchRollYaw-Knee-PitchRoll Leg Model (Fig. 3(C)). Both models consist of two rigid links. In leg model (a), the hip and knee joints rotate around the roll axis, Φ_{Roll} and Ψ_{Roll} , respectively (Fig. 4(A)). In leg model (b), the hip joint moves around the pitch, roll, and yaw axes, while the knee joint rotates around the pitch and roll axes, Φ_{Roll} , Φ_{Pitch} , Φ_{Yaw} , Ψ_{Roll} , and Ψ_{Pitch} (Fig. 4(B)). When the knee joint flexes around the pitch axis, the lengths of the anterior cruciate ligament and posterior cruciate ligament change (Li et al., 2004). However, in this study, we focus only on the knee stiffness around the roll axis, which is set to 100 N/rad. The damping of both the hip and knee joints is set to 0.1 Nm/deg/s (Herman, 2009). At around 0 degrees of shin flexion relative to the thigh, the rotational point of the knee joint around the roll axis is located about 32.6% of the distance from the lateral to the medial epicondyle (Dhaher and Francis, 2006). The Contact model between the leg and the ball is expressed as $s(d, w) \cdot (k \cdot d)$, where $s(d, w)$ is a function that monotonically increases from 0 to 1 as the penetration d is less than the transition region width w . We set w to 10^{-4} m and the ball stiffness k to 100 N/m.

3.3 Workflow of Reinforcement Learning

We made a DDPG agent using the Simulink Reinforcement Learning Toolbox (MATLAB 2024a, The MathWorks, Inc., Natick, Massachusetts, United States). We used DDPG, one of the actor-critic methods, because actor-critic methods can explore the continuous actions (Grondman et al., 2012). To further explore the actions, we set the StandardDeviation to

1 and the StandardDeviationDecayRate to 0, increasing the amount of noise in Ornstein-Uhlenbeck Action Noise. Regarding the environment setup, the leg initially starts in a straight position to the ground, with no angular velocity, while the ball is situated at 0.55 m from the leg and has velocity to move horizontally toward the leg. To let the ball hit to the leg, we applied a pulse input of 134 force toward the ball for 3 ms using the External Force and Torque block in Simulink. The time step for the simulation was set to 0.1 s.

3.3.1 Hip-Roll-Knee-Roll Leg Model

The DDPG agent (Lillicrap et al., 2019) outputs a continuous action of torque around the hip joint in the roll axis, $\tau_{Roll-hip}$, based on observations such as the thigh angle Φ_{Roll} , shin angle Ψ_{Roll} , ball position X_{Ball} , and ball velocity V_{Ball} (Fig. 4(A)). The reward for action is set as follows:

$$R = \begin{cases} 10V_{Ball} - t - 100 & \Phi_{Roll} \notin (-23^\circ, 46^\circ) \\ 10V_{Ball} - t & \Phi_{Roll} \in (-23^\circ, 46^\circ) \end{cases} \quad (8)$$

where V_{Ball} represents the current velocity of the ball when it leaves the ball, and t is the current simulation time. Each episode ends when the ball position reaches a distance of 0.8250 m from the leg or when the number of thigh swings reaches to 10 times. The torque around the hip joint ranges between -76 N·m and 112 N·m (Lanza et al., 2021) (Table 2). The optimization algorithms for optimizing the loss of both the actor and critic were Adam (Adaptive movement estimation).

3.3.2 Hip-RollPitchYaw-Knee-RollPitch Leg Model

The DDPG agent outputs continuous actions of torque around the hip joint in the pitch $\tau_{Pitch-hip}$, roll τ_{Roll} , yaw τ_{Yaw} axes, as well as around the knee joint in the pitch axis $\tau_{Pitch-knee}$ based on observations such as the thigh angle Φ_{Pitch} , Φ_{Roll} , Φ_{Yaw} , the shin angle Ψ_{Pitch} , ball position X_{Ball} , and ball velocity V_{Ball} (Fig. 4(B)). We assume that we do not change anything depend on the knee ligament condition when policy is built. Additionally, to enhance learning efficiency, we did not employ the knee joint roll angle Ψ_{Roll} for obser-

uations. The reward for the actions is set as follows:

$$R = \begin{cases} 15V_{Ball} - t - 200 & \begin{aligned} &\Phi_{Pitch} \notin (-132^\circ, 15^\circ) \\ &\Phi_{Roll} \notin (-46^\circ, 23^\circ) \\ &\Phi_{Yaw} \notin (-38^\circ, 46^\circ) \\ &\Psi_{Yaw} \notin (0^\circ, 154^\circ) \end{aligned} \\ 15V_{Ball} - t & \begin{aligned} &\Phi_{Pitch} \in (-132^\circ, 15^\circ) \\ &\Phi_{Roll} \in (-46^\circ, 23^\circ) \\ &\Phi_{Yaw} \in (-38^\circ, 46^\circ) \\ &\Psi_{Yaw} \in (0^\circ, 154^\circ) \end{aligned} \end{cases} \quad (9)$$

where V_{Ball} represents the current velocity of the ball when it leaves the leg, and t is the current simulation time. Each episode ends when the ball position reaches a distance of 0.8250 m from the leg or when the number of thigh swings reaches to 10 times. The torque around the hip joint in the pitch, roll and yaw axes ranges from $-105 \text{ N}\cdot\text{m}$ to $158 \text{ N}\cdot\text{m}$, from $-112 \text{ N}\cdot\text{m}$ to $76 \text{ N}\cdot\text{m}$, and from $-84 \text{ N}\cdot\text{m}$ to $67 \text{ N}\cdot\text{m}$, respectively (Lanza et al., 2021)(Lindsay et al., 1992)(Pontaga, 2004)(Dibrezzo et al., 1985).

4 RESULTS AND DISCUSSIONS

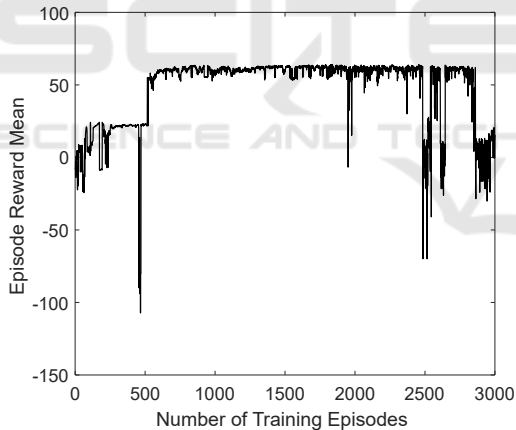


Figure 5: Episode Reward Mean for (a) Hip-Roll-Knee-Roll Leg Model.

4.1 Hip-Roll-Knee-Roll Leg Model

We trained the DDPG agent for 3000 episodes to ensure the reward had converged and the episode reward mean converged around 500 episodes (Fig. 5). In episode 3000, the agent applies a torque of $61.8 \text{ N}\cdot\text{m}$ at 0 s, which reduces to $-68.9 \text{ N}\cdot\text{m}$ and then gradually increases to $57.6 \text{ N}\cdot\text{m}$ until the leg strikes the ball at 0.49 s (Fig 7(C)). This torque sequence causes the leg to move forward, then backward, and forward again, which is pulling the thigh backward diagonally

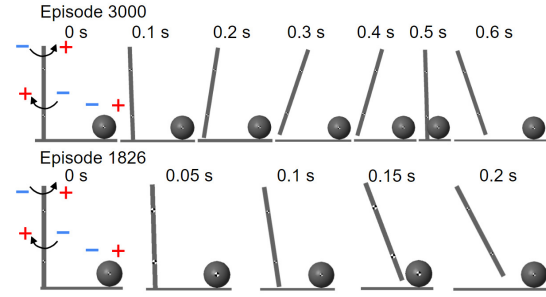


Figure 6: Motion snapshots of model (a) at 3000 and 1826 episode.

(Fig. 6, Fig 7(A)). During this motion, the shin's roll angle oscillates due to ligament elasticity, which allows the ligaments to hold potential energy until the leg makes contact with the ball (Fig 7(B)). Pulling the thigh backward diagonally causes this oscillation and contributes to the onset of energy flow. After the leg strikes the ball at 0.49 s, the hip torque around the roll axis decreases, corresponding to the stopping the thigh's acceleration. This deceleration facilitates the transfer of energy from the thigh to the shin. Additionally, it induces knee roll oscillation during contact. The ball velocity reaches 6.13 m/s.

In 1826 episode, which achieved the highest Episode Reward Mean, the agent applied a torque to swing the leg to the ball with $110 \text{ N}\cdot\text{m}$ at 0.098 s. This torque was reduced to $8.32 \text{ N}\cdot\text{m}$ at 0.18 s when the leg contacts the ball (Fig. 7(F)). This reduction in torque corresponds to stopping the thigh's acceleration (Fig 7(F)), enabling kinetic energy transfer from the thigh to the shin and inducing oscillation of the knee joint around roll axis (Fig 7(E)). Unlike 3000 episode, the hip joint angle increases monotonically, and we did not observe the pulling the thigh backward diagonally (Fig 7(D)). The ball's velocity was 6.57 m/s when the leg lost contact.

4.2 Hip-RollPitchYaw-Knee-RollPitch Leg Model

We tuned the hyperparameters (actor and critic learning rates and discount factor) using Bayesian optimization in the Simulation Manager of MATLAB. We set the actor learning rate, critic learning rate, and discount factor in the range between 10^{-3} and 1. We set the metrics EpisodeReward to maximize it with a maximum number of 30 trials. We tested two sets of hyperparameters (Table 3). In the first set, we did not observe the reward convergence while observe it in the second set (Fig. 9). For the second set of tuned hyperparameters, We tuned the hyperparameters inserting a Minibatch normalization layer between the fully

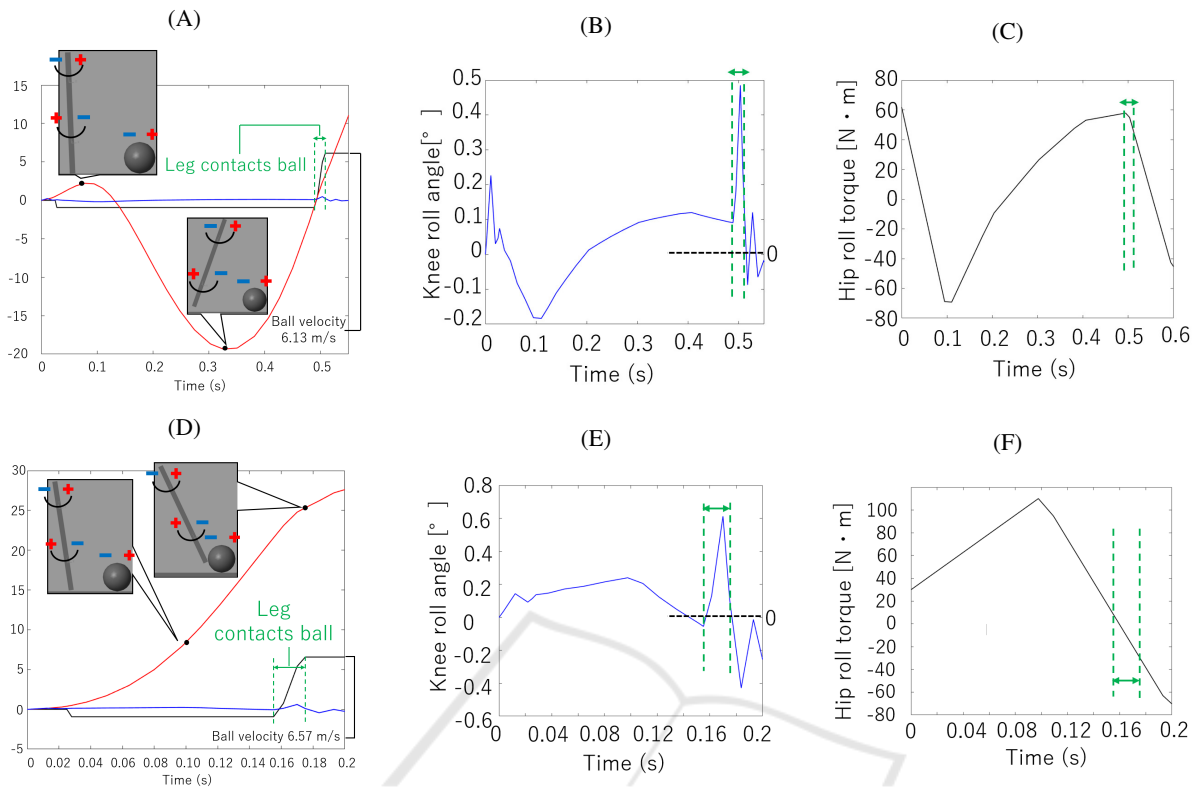


Figure 7: Ball velocity (black, (A)), thigh roll angle (red, (A)) and shin roll angle (blue, (A)(B)), along with hip roll torque (black, (C)), at the 3000 episode. Same parameters at the 1826 episode for (D),(E), and (F) in the (a) leg model. The leg makes contact with the ball between the green dotted lines.

Table 3: Tuned hyperparameters.

	Actor learning rate	Critic learning rate	Discount factor	Tuning with/without Batch Normalization
1	0.0712	0.0014	0.2440	Without
2	0.0014	0.0017	0.8534	With

Table 4: Ball velocity at 1826 episode of model (a) and at 2127 episode of model (b).

1826 episode (Model (a))	2127 episode (Model (b))
6.57 m/s	6.39 m/s

connected layer and the nonlinear functions, Relu and Tanh function.

In 3000 episode, the shin pitch torque starts at 12.7 N·m, increases to 26.1 N·m at 0.1 s, and then decreases to 9.87 N·m by 0.15 s. The hip roll torque begins at -22.2 N·m, decreases to -111.5 N·m at 0.1 s, and then rises to -30.2 N·m at 0.15 s (Fig. 8(I)). This corresponds to the stopping the thigh’s acceleration, causing the knee joint to rotate around the roll axis. The leg makes contact with the ball at the equilibrium angle of 0 deg ((Fig. 8(H))). The hip yaw torque starts at -14.6 N·m, decreases to -21.3 N·m at 0.1 s, and then rises to 6.08 N·m at 0.15 s. This

enables the foot to head outward as the knee joint extends (Fig. 10). We did not observe pulling the thigh backward diagonally and the stretching the knee suddenly. The ball velocity reaches 5.84 m/s.

In 2127 episode, which achieved the highest Episode Reward Mean, the shin pitch torque started at 5.21 N·m, increased to 22.8 N·m at 0.1 s, and then decreased to 9.73 N·m by 0.15 s. The hip roll torque began at -20.1 N·m, decreased to -111.8 N·m at 0.1 s, and then increased to -34.6 N·m at 0.15 s. This reduction corresponds to stopping the thigh’s acceleration. (Fig. 8(L)). This action allows the kinetic energy to transfer from the thigh to the shin, causing the knee joint to oscillate around the roll axis (Fig. 8(K)). The leg makes contact with the ball at the equilibrium angle of 0 deg. The hip pitch torque started at 1.75 N·m, decreasing to -31.0 N·m at 0.20 s. This facilitates the internal rotation of the foot as the knee

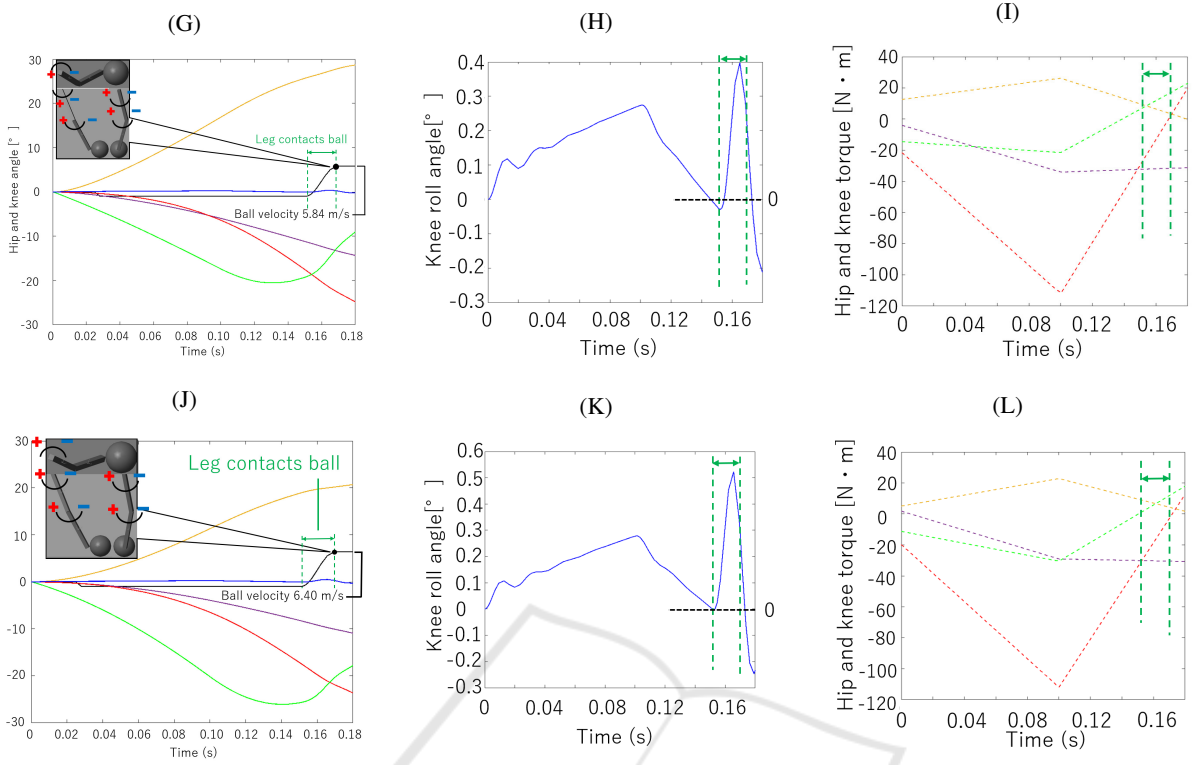


Figure 8: Ball velocity (black, (G)), thigh roll angle (red, (G)), thigh pitch angle (purple, (G)), thigh yaw angle (green, (G)), shin roll angle (blue, (G) and (H)), shin pitch angle (yellow, (G)), along with hip roll torque (red, (I)), hip pitch torque (purple, (I)), hip yaw torque (green, (I)), and knee pitch torque (yellow, (I)) at the 3000 episode. The same parameters are presented for the 2127 episode in (J),(K), and (L) for the (b) leg model. The leg makes contact with the ball between green dotted lines.

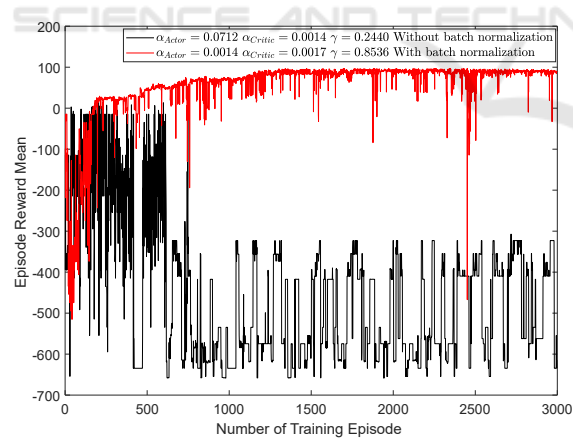


Figure 9: Episode Reward Mean for (b) Hip-RollPitchYaw-Knee-RollPitch Leg Model.

joint extends. The hip joint angles increased monotonically (Fig. 8(J)), and we did not observe pulling the thigh backward diagonally and the stretching the knee suddenly. The ball velocity reached 6.39 m/s. Furthermore, we compared the ball velocity in 1826 episode of model (a) and 2127 episode of model (b), the model (a) which leverages the stiffness of collat-

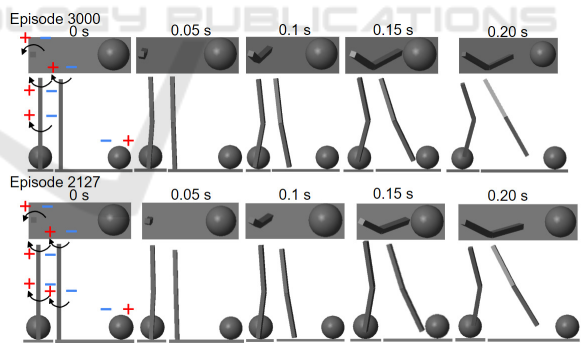


Figure 10: Motion snapshots of model (b) at 3000 and 2127 episode.

eral ligaments, produced a faster ball kick than the model (b)(Table 4). Between the Fig. 7(E) and Fig. 8(K), the knee roll angle oscillates similarly; however, the interaction phases differ. In the Fig. 8(K), the leg makes contact with the ball at approximately 0 deg, while in the Fig. 7(E), the leg exceeds 0 deg, oscillating around the equilibrium angle of the knee. This joint oscillation, driven by the ligaments, affects on the ball velocity. These results suggest that utilizing collateral ligaments leads to a faster ball.

5 CONCLUSION

We confirmed that the agent developed strategies similar to an outside pass in soccer. For the leg model (a), episode 1826 showed stopping the thigh's acceleration while did not show pulling the thigh backward diagonally. 3000 episode included both. In contrast, leg model (b) demonstrated bending the knee and stopping the thigh's acceleration at episodes 2127 and 3000, while we did not observe the pulling the thigh backward diagonally and stretching the knee suddenly. Additionally, we observed that the leg model (a), which utilizes the collateral ligaments' stiffness, resulted in a faster ball compared to leg model (b), which is capable of moving in directions that do not engage the collateral ligaments' stiffness. We achieved better understanding of the joint strategies in an outside pass where ligaments involve, which is beneficial for developing strategies to kick faster ball with small motion. For future work, we aim to investigate whether oscillation around the roll axis of the knee joint occurs in human. Additionally, we plan to further explore strategies involving muscle strengthening and knee joint oscillation in other sports, such as tennis and volleyball.

REFERENCES

- Aeles, J. and Vanwanseele, B. (2019). Do stretch-shortening cycles really occur in the medial gastrocnemius? a detailed bilateral analysis of the muscle-tendon interaction during jumping. *Front Physiol*.
- Asaoka, T. and Mizuuchi, I. (2017). Generation of the swing motion pattern of a multi-link robot for the explosive increase of the kinetic energy of the end-link by exploiting dynamic coupling. *Transactions of the JSME (in Japanese)*.
- Cerrah, A. O., Gungor, E. O., Soylu, A. R., Ertan, H., Lees, A., and Bayrak, C. (2011). Muscular activation patterns during the soccer in-step kick. *Isokinetics and Exercise Science*.
- Chiras, D. D. (2018). *Human Biology*. Jones Bartlett Learning.
- Christenson, A. J. and Casa, D. J. (2020). Analysis on the effect of ball pressure on head acceleration to ensure safety in soccer. *Proceedings*.
- Dhaher, Y. Y. and Francis, M. J. (2006). Determination of the abduction-adduction axis of rotation at the human knee: helical axis representation. *Journal of orthopaedic research : official publication of the Orthopaedic Research Society*.
- Dibrezzo, R., Gench, B. E., Hinson, M. M., , and King, J. (1985). Peak torque values of the knee extensor and flexor muscles of females. *The Journal of orthopaedic and sports physical therapy*.
- Fukasawa, S. (2000). Biomechanics in stretch-shortening cycle exercise. *Japanese Society of Physical Education*.
- Grondman, I., Busoniu, L., Lopes, G. A. D., and Babuska, R. (2012). A survey of actor-critic reinforcement learning: Standard and natural policy gradients. *IEEE Transactions on Systems, Man, and Cybernetics, Part C (Applications and Reviews)*.
- Herman, I. P. (2009). *Physics of the Human Body Biological and Medical Physics, Biomedical Engineering*. NTS.
- Ho-Jung, C. and Dai-Soon, K. (2020). Mechanical properties and characteristics of the anterolateral and collateral ligaments of the knee. *Applied Sciences*.
- Hondo, T. and Mizuuchi, I. (2012). Realization method of high kinetic energy utilizing elastic joints based on feedback excitation control and analysis of equal energy hypersurfaces. *Proceedings of the 2012 JSME Conference on Robotics and Mechatronics*.
- Ishii, H., Yanagiya, T., Naito, H., Katamoto, S., and Maruyama, T. (2009). Numerical study of ball behavior in side-foot soccer kick based on impact dynamic theory. *J Biomech*.
- Ker, R. F., Bennett, M. B., Bibby, S. R., Kester, R. C., and Alexander, R. M. (1987). The spring in the arch of the human foot. *Nature*.
- Kozo, N. and Takeo, M. (2006). A 3d dynamical model for analyzing the motion-dependent torques of upper extremity to generate throwing arm velocity during an overhand baseball pitch. *Jpn J Biomechanics Sports Exerc*.
- Kozo, N., Yosuke, F., and Takeo, M. (2007). Analysis of mechanical energy generation, transfer and causal energy sources in soccer instep kick. *The Proceedings of Joint Symposium: Symposium on Sports Engineering, Symposium on Human Dynamics*.
- Lanza, M. B., Rock, K., Marchese, V., Addison, O., and Gray, V. L. (2021). Hip abductor and adductor rate of torque development and muscle activation, but not muscle size, are associated with functional performance. *Frontiers in Physiology*.
- Levin, A., Wyman, J., and Hill, A. V. (1927). The viscous elastic properties of muscle. *Proceedings of the Royal Society of London. Series B, Containing Papers of a Biological Character*.
- Li, G., DeFrate, L. E., Sun, H., and Gill, T. J. (2004). In vivo elongation of the anterior cruciate ligament and posterior cruciate ligament during knee flexion. *The American journal of sports medicine*.
- Lillicrap, T. P., Hunt, J. J., Pritzel, A., Heess, N., Erez, T., Tassa, Y., Silver, D., and Wierstra, D. (2019). Continuous control with deep reinforcement learning. *arXiv*.
- Lindsay, D. M., Maitland, M., Lowe, R. C., and Kane, T. J. (1992). Comparison of isokinetic internal and external hip rotation torques using different testing positions. *Journal of Orthopaedic & Sports Physical Therapy*.
- Nagurka, M., , and Huang, S. (2004). A mass-spring-damper model of a bouncing ball. *Proceedings of the 2004 American Control Conference*.
- Pontaga, I. (2004). Hip and knee flexors and extensors bal-

- ance in dependence on the velocity of movements. *Biology of Sport*.
- Senoo, T., Namiki, A., and Ishikawa, M. (2008). High-speed throwing motion based on kinetic chain approach. *2008 IEEE/RSJ International Conference on Intelligent Robots and Systems*.
- Tomohisa, M., Norihisa, F., Michiyoshi, A., Yasuo, K., and Morihiko, O. (1997). A three-dimensional analysis on mechanical energy flows of torso and arm segments in baseball throw. *Japanese Journal of Physical Fitness and Sports Medicine*.
- Wiesinger, H. P., Rieder, F., Kösters, A., Müller, E., and Seynnes, O. R. (2017). Sport-specific capacity to use elastic energy in the patellar and achilles tendons of elite athletes. *Front Physiol*.
- Woo, S. L., Johnson, G. A., and Smith, B. A. (1993). Mathematical modeling of ligaments and tendons. *Journal of Biomechanical Engineering*.
- Xu, C., Ming, A., Maruyama, T., and Shimojo, M. (2007). Motion generation for hyper dynamic manipulation. *Mechatronics*.

